

Relativistic and relaxation effects in the near-edge K photoabsorption of xenon and radon

J. Tulkki

Laboratory of Physics, Helsinki University of Technology, SF-02150 Espoo, Finland

(Received 22 July 1985)

The relativistic photoabsorption cross section in the vicinity of the xenon and radon K -absorption edges is calculated using the Dirac-Fock method. The relaxation is included by constructing separate solutions for the initial ground state and for the final $1s$ -hole state and by including the resulting overlap integrals into the transition amplitude. The relativistic effect is found to lower the cross section with 12% and 35% for xenon and radon, respectively. One-third of this effect results from the change in the K -ionization energy and two-thirds from the change in the wave functions. The full overlap correction is shown to increase the cross section by a factor of 2 in the threshold region. The influence of the postcollision effect on the xenon K cross section was found to be negligible. The cross sections are shown to be nearly gauge invariant with the $E1$ multipole dominating. In radon the higher multipoles contribute with 4%.

INTRODUCTION

Prompted by a controversy over the near-edge behavior of the inner-shell photoabsorption cross sections,^{1,2} we have recently reported a thorough study of photoionization in the vicinity of the argon K -absorption edge.³ The detailed form of the atomic photoabsorption cross sections in the threshold region is of fundamental importance because of its usefulness as a reference spectrum in the extended x-ray-absorption fine-structure (EXAFS) and x-ray-absorption near-edge-structure (XANES) spectroscopies. In our work³ we showed that the deviations from the monotonic decrease in the cross section predicted by Manson and Inokuti¹ are most evidently caused by the numerical procedure in obtaining the photoelectron wave function. Furthermore, it was shown that the effect of the postcollision interaction (PCI) on the K -photoabsorption is small in contrast to results by Amusia, Ivanov, and Kupchenko,² who found PCI decisive at threshold.

In this work we consider the K -photoabsorption edges of xenon and radon with special emphasis on relativistic effects in conjunction with relaxation and PCI. The relativistic K -photoabsorption cross sections have been calculated earlier by Scofield⁴ by use of the Dirac-Slater model, but he did not consider the near-edge behavior in detail. For high photon energies⁵ various one-electron models have been used to calculate the photoabsorption cross sections. In these models the screening, exchange, and correlation effects are accounted for parametrically, which does not make them suitable for the analysis of the near-edge behavior of the spectrum.

THEORY

The relativistic photoabsorption cross sections were calculated by the Dirac-Fock (DF) method by use of a continuum program implemented to the multiconfiguration DF program package by Grant *et al.*⁶ The relativistic continuum wave functions of the photoelectrons ϵ_l , $l=0,1,2$, and $j=\frac{1}{2}-\frac{5}{2}$ were calculated by keeping the bound orbitals fixed for the given core configuration. The Lagrangian multipliers technique was used to enforce orthogonality between

bound orbitals and the continuum orbital. Consequently, the wave function of the photoelectron is obtained by iteratively solving the equations

$$\frac{dP}{dr} + \frac{\kappa}{r}P - \left[2c + \frac{1}{c} \left(\frac{Y(r)}{r} + \epsilon \right) \right] Q = \xi(r), \quad (1)$$

$$\frac{dQ}{dr} - \frac{\kappa}{r}Q + \frac{1}{c} \left(\frac{Y(r)}{r} + \epsilon \right) P = \eta(r).$$

In Eq. (1) P and Q are the large and small radial components of the four spinors. The nuclear attraction and direct electron-electron repulsion are included in Y , whereas the nonlocal exchange potentials are given by ξ and η . Equation (1) has been discussed in detail by Grant.⁷ For the normalization of the continuum wave function we used the orthodox procedure⁸ of fitting the numerical solution to a linear combination of the regular and irregular solutions of the Coulombic Dirac equation outside the ion. In particular, the Coulombic solutions were calculated without the asymptotic approximation by use of a special numerical approach, which enables an accurate evaluation of pertinent Whittaker functions also at distances of a few atomic units. Therefore, our cross sections are free from any artifacts caused by inaccurate normalization.

The calculation of the transition amplitude is based on the covariant electron-photon interaction $H_I = -c\gamma^\mu A_\mu$, which gives in the first-order perturbation theory and single configuration and channel approximation the photoabsorption cross section (in atomic units)

$$\sigma_K(\omega) = \frac{2\pi^2}{3\alpha\omega} \sum_{fL\xi} |\langle \Psi_{\epsilon,f} | \alpha \cdot \sum_{\nu} [A_L^{(\xi)}(\mathbf{r}_\nu) + GA_L^{(0)}(\mathbf{r}_\nu)] | \Psi_i \rangle|^2, \quad (2)$$

where Ψ_i and $\Psi_{\epsilon,f}$ are the initial and final many-electron wave functions of the absorbing atom, respectively. The index L gives the rank of the multipole and ξ denotes the magnetic ($\xi=m$) and electric ($\xi=e$) multipoles. The gauge transformations are included by the parameter G which obtains the values 0 and $1/\sqrt{2}$ for the Coulomb

(velocity) and length gauges, respectively. The retardation is taken into account by the energy dependence of the Bessel functions in the transition operators. For the detailed definition of the multipole operators see Grant.⁹ In the case of xenon, only the electric dipole ($E1$) transition was considered, whereas for radon we also included magnetic dipole ($M1$) and electric and magnetic quadrupole ($E2, M2$) transitions. The nonorthogonality of the initial and final basis sets was taken into account using Scofield's¹⁰ formulation. For that purpose the reduced one-electron and overlap matrix elements were first calculated using formulas given by Grant.⁹ The summation over the various products of overlap integrals and one-electron amplitudes was then performed using an efficient computer code.

RESULTS AND DISCUSSION

The cross sections were calculated using both local Kohn-Sham exchange and full nonlocal exchange potentials. Since the cross sections obtained in various local approximations were qualitatively similar to those reported earlier for argon,³ we have only plotted the cross sections calculated using ground-state orbitals for both the initial and final states in order to compare with Scofield's⁴ results. As in the case of argon, this approximation involves the Latter's tail correction in the asymptotic region, which, because of the discontinuity in the derivative of the potential, causes the weak oscillating behavior shown in Figs. 1 and 2. Although Scofield's tables do not include information on the near-edge behavior, his values at thresholds 5.79 and 1.67 kb for xenon and radon, respectively, are in perfect agreement with our results.

The calculation with the nonlocal exchange potential was done by calculating separate bound-state wave functions for the initial and final states. For radon we used a potential with a uniformly charged finite nucleus in the calculation of both the bound and continuum orbitals. The finite-nucleus

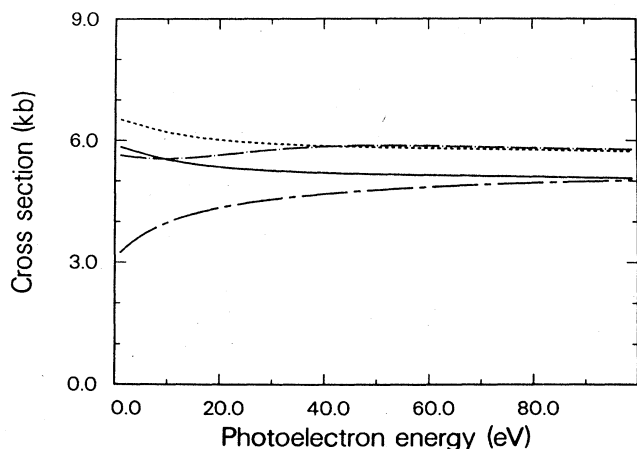


FIG. 1. The K -photoabsorption cross sections for xenon in electric dipole approximations. The solid line represents the Dirac-Fock cross section including full relaxation. The chain-dashed line represents the same as the solid line, but without the overlap corrections. The chain-dotted line represents Dirac-Slater with ground-state orbitals and Latter's tail correction. The dashed line represents the nonrelativistic cross section including full relaxation.

correction was, however, found to be small, because of the low photoelectron energies. The transition amplitudes were calculated for xenon in the electric dipole approximation, but for radon we also calculated the magnetic dipole and electric and magnetic quadrupoles which contributed at the threshold with 1.5, 64, and 5 b, respectively. In the full relaxation calculation all the resulting one-electron overlap integrals were included in the transition amplitude. The results are given by solid lines in Figs. 1 and 2. The cross sections were calculated both in the velocity and length gauge, which were found to differ at most of the order of one percent.

We also calculated the nonrelativistic cross sections including full relaxation. This was achieved by using the same Dirac-Fock equations and electron-photon coupling as above, but with the velocity of light multiplied by a factor of 1000. Since the electronic configurations involved include only s -like open shells, our procedure gives the unique nonrelativistic limit. The nonrelativistic cross sections which were calculated using the nonrelativistic K -shell ionization energy are given by dashed lines in Figs. 1 and 2. In order to distinguish between relativistic energy and orbital effects, we also calculated these cross sections with the relativistic ionization energy. The result shows in the case of radon that the energy shift covers one-third of the relativistic effect. The relativistic orbital contraction was investigated by constructing the effective total and exchange potentials of the ionized electron. The most physical approach would be to apply the phase-amplitude method,¹¹ but no proper reformulation for the nonlocal potential exists. Hence we plotted the potentials

$$\begin{aligned} V_{\text{eff}} &= Y(r) + V_{\text{exch}}, \\ V_{\text{exch}} &= -cr\xi(r)/Q(r), \end{aligned} \quad (3)$$

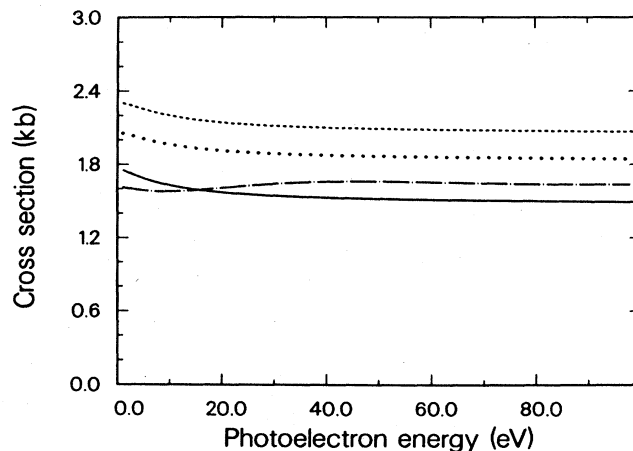


FIG. 2. The relativistic and nonrelativistic photoabsorption cross sections at the radon K -absorption edge. All the nonlocal cross sections include full relaxation. The solid line represents the Dirac-Fock cross section. The chain-dotted line represents the Dirac-Slater approximation with ground-state orbitals and Latter's tail correction. The dashed line represents the nonrelativistic cross section. The dotted line was obtained using nonrelativistic wave functions but relativistic K -ionization energy. The relativistic cross section includes also the contributions from the magnetic dipole and electric and magnetic quadrupole transitions, which contribute altogether about 4%.

which effectively determine the large radial component of the continuum orbital. The potentials, as well as the photoelectron wave functions, are given in Fig. 3. The relativistic results are represented by the solid line. The one-electron wave functions plotted are actually the large components which in the nonrelativistic case are equal to the radial part of the wave function. In the relativistic case the continuum orbital refers to the $j = \frac{3}{2}$ component. Note, however, that the relativistic $j = \frac{1}{2}$ and $\frac{3}{2}$ orbitals are quite similar, as demonstrated by the fact that the beta parameter¹² describing the angular photoelectron distribution is very close to two for both considered atoms. The most prominent feature in Fig. 3 is the overall relativistic contraction bringing the electrons closer to the nucleus. The changes are significant both in the $1s$ and continuum orbital. The variation in the exchange interaction is more complicated. If the exchange potential is assumed to be approximately proportional to a fractional power of the electron density the shift to its local minima towards zero is also in accordance with the relativistic contraction phenomenon.

For xenon we also estimated the influence of PCI on the cross section.¹³ The numerical procedure in this calculation was nearly similar to that used in the case of argon.³ In contrast to argon, the probability for recapture of the photoelectron into Rydberg states was found to be significant for excess energies up to 30 eV. The PCI distortion of the *KLL* Auger lines was considerable, resulting in an energy shift from 3 to 2.5 eV for excess energies from 10 to 50 eV, comparable to the shift found recently for xenon *LLM* Auger lines by Armen *et al.*¹⁴ The influence of PCI on the photoabsorption cross section was, however, negligible. The reason is that the radiative mode dominates the *K*-shell hole decay in xenon. The radiative PCI effect is most evidently small, although no direct calculations exist.

In conclusion, we have shown that the relativistic effects at the *K*-photoabsorption edge become important already for xenon, for which they contribute with 12%. In radon the relativistic correction at the absorption edge is 36%. The in-

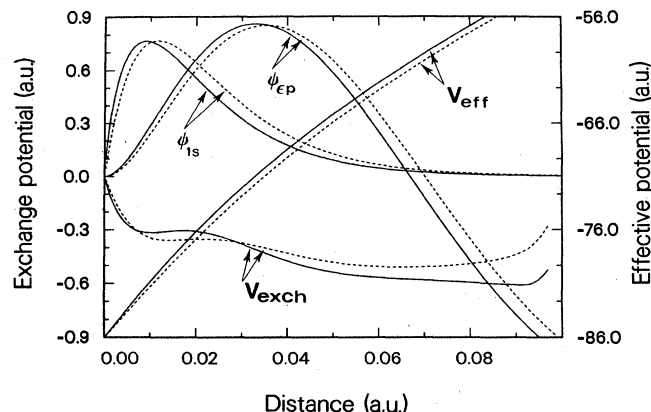


FIG. 3. The exchange and effective total potentials seen by the photoelectron in the near-edge *K* photoabsorption in radon. The relativistic and nonrelativistic results are given by solid and dashed lines, respectively. The one-electron initial $1s$ and final ϵp_j orbitals ($j = \frac{3}{2}$ in the relativistic case) are also given. See text for a detailed definition of the given potentials. The kinetic energy of the continuum electron is 10 eV.

clusion of the full overlap correction increases the cross section by a factor of 2 in the threshold region. As in the case of argon³ this exchange-induced relaxation effect results from dipole excitations of the $1s$ electron to initially occupied np_j states, followed by monopole ionization to ϵp_j states. Altogether, these amplitudes contribute with 31–33% to the total transition amplitude. Analogous effects were also found for higher multipoles in radon. The experimental data presently at hand do not allow for a direct comparison with our theoretical results, since such a comparison is possible only below the double ionization threshold. Therefore, the need of synchrotron-radiation measurements of the absorption near the *K* edges is apparent.

¹S. T. Manson and M. Inokuti, *J. Phys. B* **13**, L323 (1980).

²M. Ya. Amusia, V. K. Ivanov, and V. A. Kupchenko, *J. Phys. B* **14**, L667 (1980).

³J. Tulkki and T. Åberg, *J. Phys. B* **18**, L489 (1985).

⁴J. H. Scofield, Lawrence Livermore Laboratory Research Report No. UCRL-51326, 1980 (unpublished).

⁵R. H. Pratt, A. Ron, and H. K. Tseng, *Rev. Mod. Phys.* **45**, 273 (1973).

⁶I. P. Grant, B. J. McKenzie, P. H. Norrington, D. F. Mayers, and N. C. Pyper, *Comput. Phys. Commun.* **21**, 207 (1980).

⁷I. P. Grant, *Adv. Phys.* **19**, 747 (1970).

⁸B. Müller, J. Rafelski, and W. Greiner, *Nuovo Cimento* **18A**, 551 (1973).

⁹I. P. Grant, *J. Phys. B* **12**, 1458 (1974).

¹⁰J. H. Scofield, *Phys. Rev. A* **9**, 1041 (1974).

¹¹U. Fano, C. E. Theodosiou, and J. L. Dehmer, *Rev. Mod. Phys.* **48**, 49 (1976).

¹²S. T. Manson and A. F. Starace, *Rev. Mod. Phys.* **54**, 389 (1982).

¹³T. Åberg, in *Inner-Shell and X-Ray Physics of Atoms and Solids*, edited by D. J. Fabian, H. Kleinpoppen, and L. M. Watson (Plenum, New York, 1981), p. 251.

¹⁴G. B. Armen, T. Åberg, J. C. Levin, B. Crasemann, M. H. Chen, G. E. Ice, and G. S. Brown, *Phys. Rev. Lett.* **54**, 1142 (1985).